Journal of Alloys and Compounds, 211/212 (1994) 216–221
JALCOM 013

Mechanical spectroscopy with hydrogen in intermetallic phases*

H.-R. Sinning
Institut für Werkstoffe, Technische Universität Braunschweig, D-38023 Braunschweig (Germany)

Abstract

On the basis of the reorientation relaxation of hydrogen in amorphous and crystalline intermetallic phases, the potential of "mechanical hydrogen spectroscopy" (MHS) as a tool for structural investigations is exemplified using $CoZr_2$ as a model alloy. After a brief overview of the related internal friction phenomena and their microscopic interpretation, it is shown by MHS (i) that, even in a nanocrystalline material produced by crystallization of a metallic glass, the structure of the grain boundaries is somewhat more "disordered" than that of the glass, and (ii) that amorphous $CoZr_2$ contains local structural elements from two different crystalline phases of the same composition. In addition, MHS may also be used on a more empirical level for characterizing microstructures and phase transformations.

1. Introduction

Anelastic relaxation produced by dissolved hydrogen in a solid matrix can be either of long-range (Gorsky) or of short-range (reorientation) type, depending on whether the isotropic or the anisotropic part respectively of the local elastic distortion field (λ tensor) is involved. For the second type, a further distinction can be made according to whether the anisotropic distortion ("elastic dipole") can be produced by a single H atom or only by some combination of defects. The subject of the following considerations is only short-range reorientation processes that can in principle be produced by single hydrogen atoms, *i.e.* processes similar to the well-known Snoek relaxation of heavier interstitials (C, N, O) in b.c.c. metals. Such processes have been observed for hydrogen in amorphous alloys [1–3] and some intermetallic compounds [4, 5], but not in pure b.c.c. metals [6, 7].

In amorphous alloys, H reorientation relaxation is a common phenomenon that has hitherto been observed in about 20 systems [1]. It manifests itself as a broad, asymmetric internal friction (IF) peak that usually shifts to lower temperatures with increasing H concentration. The properties of this peak (*e.g.* distribution of activation energies) reflect the atomic disorder of the amorphous matrix, the occupation of interstitial sites (often identified as tetrahedral sites, *e.g.* in the case of transition metal glasses [8]) according to Fermi–Dirac statistics [9], and the thermally activated jump of the H atoms over saddle point barriers [10]. However, the development of a detailed, quantitative model of the H reorientation relaxation in amorphous alloys is still a matter of debate [11–13] which will be discussed in a separate paper [14].

In crystalline intermetallic compounds, there are as yet only a few manifestations of an H reorientation relaxation. After the discovery of H-induced IF peaks in Nb_3Sn [15] and in two crystallized glasses [16, 17], the first observations that were clearly attributed to specific atomistic mechanisms were, independently of each other, those by Sobha *et al.* [4] on Pd_3Mn and by Sinning [5] on tetragonal (C16 phase) $CoZr_2$. The latter work was followed by a theoretical treatment of the relaxation process in the C16 compounds resulting in quantitative relationships, *e.g.* between lattice parameters and activation energies [18], and also by further experimental results on different stable and metastable $CoZr_2$, $NiZr_2$ and $NiTi_2$ phases and microstructures [19–21].

On the basis of such reorientation relaxation processes of hydrogen in amorphous and crystalline intermetallic phases, the purpose of the present paper is to exemplify the potential of mechanical spectroscopy, in the sense of a tool for structural and microstructural investigations. The experimental background for these considerations is mainly IF results on $CoZr_2$ which for this purpose represents an excellent model alloy.

2. The model alloy $CoZr_2$: results and basic ideas

As described in detail elsewhere [5, 19, 20], the H-induced IF spectra of melt-spun $CoZr_2$ ribbons were measured with the vibrating reed technique for H concentrations [H]/[M] between 0.001 and about 1 (ratio

*Invited paper.

SSDI 0925-8388(93)00013-O

of hydrogen to metal atoms). The alloy $CoZr_2$ was chosen because its crystallization sequence is particularly rich in different structures with the same chemical composition, including complex cubic ($E9_3$, $NiTi_2$ type), hexagonal (similar to $Ce_{24}Co_{11}$ type [22]) and tetragonal (C16, $CuAl_2$-type equilibrium phase) crystals [24–27]. (The hexagonal phase was first found by Köster *et al.* [23] in rapidly heated samples; in our conventionally heated samples, lattice parameters $a = 8.753$ Å and $c = 19.385$ Å were determined from X-ray diffraction. With 70 atoms cell^{-1} and almost the same c/a ratio this structure looks similar to that of $Ce_{24}Co_{11}$ (space group $P6_3mc$, Pearson symbol hP70 [22]), but a complete structure determination has not yet been possible.) The first stage in this sequence is a metastable, nanocrystalline [27] state of the cubic $E9_3$ phase; the second, hexagonal metastable phase only appears in a complicated, multiphase "mixed state" before it finally transforms into the equilibrium phase.

As shown in Figs. 1 and 2, each phase in this transformation sequence exhibits a characteristic IF peak; these peaks were all explained as H reorientation peaks with the H atoms jumping between the following sites [5, 19, 20]: peak 1, amorphous phase, Zr_4 tetrahedra at low to intermediate and Zr_3Co tetrahedra at high H concentrations; peak 2 (low H concentrations), Zr_4 tetrahedra in the grain boundaries of the nanocrystalline state; peak 2′ (high H concentrations), Zr_3Co tetrahedra in the cubic $E9_3$ structure; peak 3, hexagonal phase, further details not yet known; peak 4, Zr_4 tetrahedra in the tetragonal C16 structure, as treated quantitatively in the above-mentioned work [18, 21].

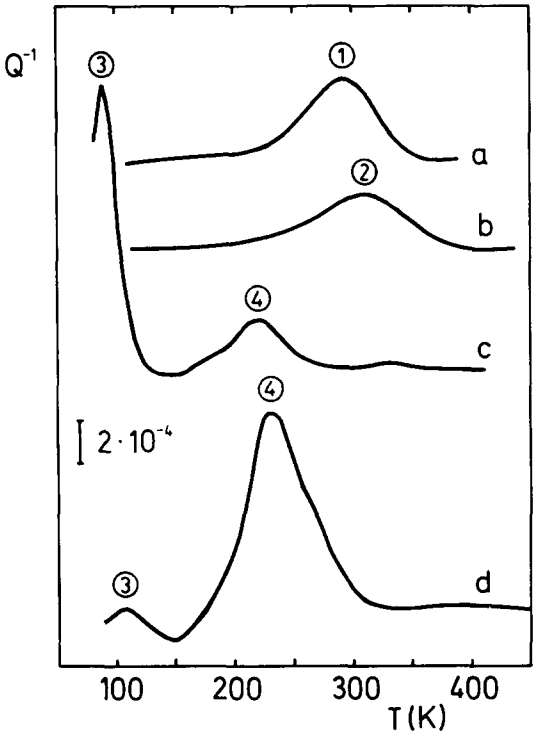

Fig. 1. Sequence of IF Q^{-1} spectra ($f = 580 \pm 80$ Hz) in $CoZr_2$ with about 0.3 at.% H ([H]/[M] = 0.003) after different heat treatments (*cf.* refs. 5 and 20): curve a, amorphous state; curve b, nanocrystalline state; curve c, intermediate mixed state (see text); curve d, transformation into the tetragonal (C16) equilibrium phase almost complete.

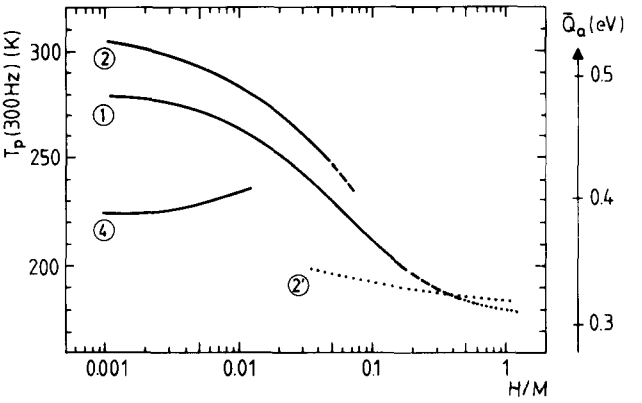

Fig. 2. Schematic drawing of the H concentration dependence of the peak temperatures T_p (for $f = 300$ Hz) of the IF peaks measured in $CoZr_2$ [19, 20]: peak 1, amorphous state; peaks 2–2′, nanocrystalline state (grain boundaries–cubic $E9_3$ crystals); peak 4, C16 equilibrium phase; ——, main contribution from Zr_4 tetrahedral sites; · · · · ·, main contribution from Zr_3Co tetrahedral sites. The right-hand activation energy scale holds for an assumed pre-exponential factor $\tau_0 = 10^{-12}$ s.

The main point to be emphasized with regard to mechanical spectroscopy (in the above sense) is that most of these relaxation processes are due to the same atomistic, local event: the thermally activated jump of the H atom between neighbouring tetrahedral sites, embedded in the corresponding amorphous or crystalline matrix structures. As long as the hydrogen–metal interaction is essentially confined to nearest neighbours (see, for example, refs. 10 and 18), there must be a unique relationship between the kinetic relaxation parameters and the local atomic arrangement around the jumping proton independent of the surrounding long-range structure (in contrast to relaxation kinetics, this conclusion does not hold for the relaxation strength which depends on the $\boldsymbol{\lambda}$ tensor and thus on the structure-dependent elastic constants). Such a relationship then offers a basis for applying the relaxation processes as a local probe to study structural details of the matrix.

As long as a direct determination of this relationship ("absolute gauge") by theory or independent experiments is not available, the only way of using it is the local comparison between structures in cases such as that of $CoZr_2$, where the same local process occurs in several different structures ("relative gauge").

Two examples will now be discussed which demonstrate what kinds of results can be obtained with this approach: a structural comparison between the grain boundaries in the nanocrystalline state and the

amorphous phase based on the properties of peaks 1 and 2, and the question of local correspondences between amorphous and crystalline structures, based on a comparison of peak 1 with the "crystalline" peaks 2′ and 4. Finally, some further, more empirical applications of "mechanical hydrogen spectroscopy" (MHS) will also be considered briefly.

3. Grain boundaries in the nanocrystalline state

The most important structural question in the expanding field of nanocrystalline materials [28] is that of the structure of the grain boundary component, which obviously depends strongly on the method of production. For nanocrystalline materials prepared by crystallization from a metallic glass as in the case of $CoZr_2$, the glassy structure seems to persist in the grain boundaries, as concluded for example from positron lifetime measurements [29], magnetic after-effect [30], and also our earlier H-induced IF measurements [5, 19, 20], where no significant difference was detected.

However, a better use of the structural sensitivity of MHS can still be made by considering the H concentration dependence of the relaxation kinetics in more detail. Since in the nanocrystalline state the H concentrations may differ between the crystals and the grain boundaries, it is not the total [H]/[M] value as in Fig. 2 but the unknown local value in the grain boundaries which should be considered.

If now the structures of the grain boundaries and the amorphous phase are at least approximately equal to each other as stated above, this must also be true for the relaxation strengths per H atom. Hence, for the purpose of comparison, the unknown local H concentration may be replaced by the measured IF peak height Q_P^{-1} divided by an appropriate volume fraction α, which has been done in Fig. 3.

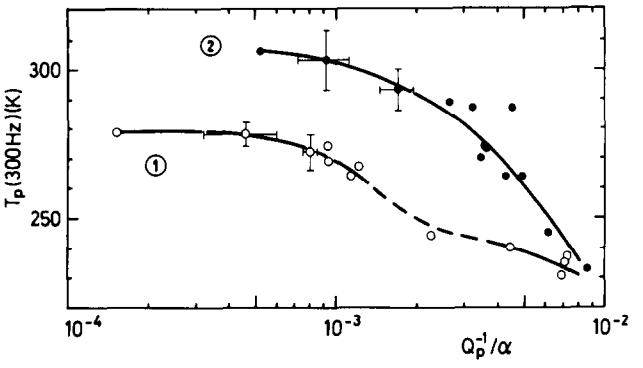

Fig. 3. The peak temperatures T_p (for $f=300$ Hz) in amorphous (peak 1) and nanocrystalline (peak 2) $CoZr_2$ as a function of the peak height Q_p^{-1}, divided by an appropriate volume fraction α (amorphous state, $\alpha=1$; nanocrystalline state, $\alpha=0.25$, volume fraction of grain boundaries [31]).

In addition, the ordinates in Figs. 2 and 3 may be read as average activation energies (assuming a constant pre-exponential factor τ_0) and reflect the local distribution of Zr–Zr distances in the sense that higher peak temperatures or activation energies correspond to sites of lower energy, with larger Zr–Zr distances.

Thus, the result of Fig. 3 indicates that on a certain change in the local H concentration, the average activation energy exhibits more variation in the nanocrystalline state, corresponding to a broader distribution of Zr–Zr distances in the grain boundaries, than in the amorphous phase. In particular, the differences at low H concentrations can be understood as the result of some larger interstitial holes in the grain boundaries.

For the class of nanocrystalline materials produced by crystallization of a metallic glass, this is possibly the first experimental indication that even in this case the structure of the grain boundaries is somewhat "more disordered" (less dense) than that of a glass.

In the light of this interpretation, the further shift of the IF peak to higher temperatures observed with increasing grain size [5, 20] can naturally be explained by an increasing difference between the grain boundary and glass structures; the same tendency is also seen for the alloys $Ni_{35}Ti_{65}$ and $Ni_{35}Zr_{65}$ [20]. Thus, MHS is obviously able to detect some subtle, gradual differences of disordered structures between the limits of a glass and a grain boundary in a polycrystalline material.

4. Local correspondences between amorphous and crystalline structures

The question of how far an amorphous structure can be described by local "structural units" from related crystalline phases has often been considered (*e.g.* refs. 32 and 33). In amorphous $CoZr_2$, we may look with MHS at the topological short-range order (TSRO) among the Zr atoms at low H concentrations and at the surroundings of the Co atoms at high H concentrations, in relation to the metastable cubic as well as the stable tetragonal phase.

With respect to TSRO among the Zr atoms, it can be stated *a priori* that there are Zr_4 tetrahedra in the amorphous [8] and tetragonal, but not in the cubic [34] phases. We shall now see that more quantitative information on the Zr–Zr distances is obtained from the corresponding IF peaks 1 and 4.

Figure 4 shows the geometry of those Zr_4 tetrahedral sites in $CoZr_2$ and $NiZr_2$ that are responsible for the H reorientation relaxation in the C16 lattice [18, 21]. It is seen that because of the four different Zr–Zr distances d_1–d_4 [35], the two tetrahedra are distorted in different crystallographic directions, but by almost

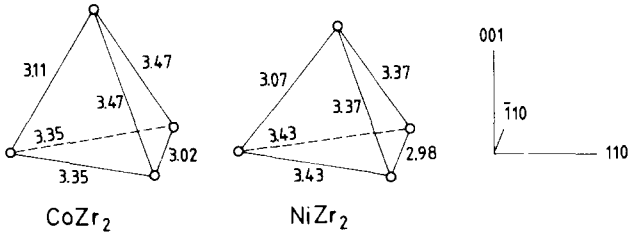

Fig. 4. The dimensions (in ångströms) of the type 2 [18] Zr_4 tetrahedra around the 16l interstitial sites in the C16 phases $CoZr_2$ and $NiZr_2$.

the same amount. The relaxation strength, however, is considerably larger in tetragonal $CoZr_2$ (Fig. 1) than in $NiZr_2$ [20], with the values for the corresponding amorphous phases between them. This seems to indicate (with some limitation; see Section 2) that also the distortions of the Zr_4 tetrahedra in amorphous $CoZr_2$ and $NiZr_2$ are of the same order of magnitude as in the C16 phases.

With respect to relaxation kinetics, it has been shown for the C16 lattice that the activation energy of the dominating reorientation jump in $CoZr_2$ is a function of d_2+2d_4 [18], which means that the value measured at dilute H concentrations is related to a Zr–Zr distance of 3.27 Å (which is the average of the three edges leading to the left-hand corner in Fig. 4).

In the amorphous structure the situation is more complicated, because different parts of the continuous distribution of Zr–Zr distances are scanned at different H concentrations. A full treatment of this problem requires a thorough, fundamental discussion of the relaxation models (see above) and the numerical application of a model structure such as that of Richards [10], which is not possible here. What can be said, however, is that there must exist a certain H concentration where the measured, average activation energy of relaxation just corresponds to the average Zr–Zr distance in the amorphous structure. From the discussion of relaxation models [14], the measured low concentration activation parameters (0.47 eV and 2×10^{-12} s for peak 1 and 0.41 eV and 3×10^{-13} s for peak 4 [5]), and the concentration dependence of peak temperatures in Fig. 2, one can roughly estimate that, at this unknown H concentration, the average activation energy in the amorphous state must be close to the low concentration value in the C16 phase. According to what has been said above, this implies an average Zr–Zr distance close to 3.27 Å in amorphous $CoZr_2$.

Assuming a gaussian distribution for the Zr–Zr distances (as often found in metallic glasses [36]), the combined results from relaxation strength and kinetics therefore suggest a mean value of 3.27 Å and a width $2\sigma=0.45$ Å (*cf.* Fig. 4) for amorphous $CoZr_2$. As shown in Fig. 5, this distribution indeed agrees very well with

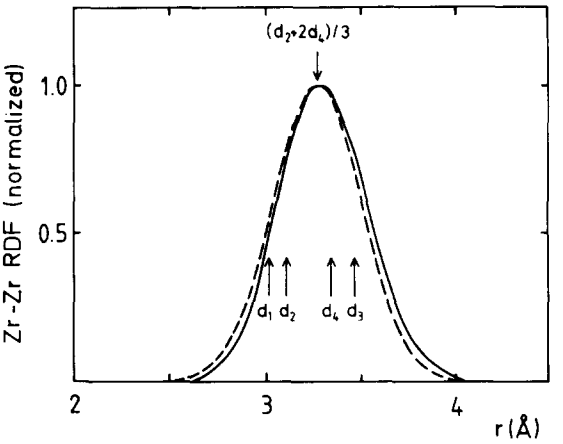

Fig. 5. Comparison of the Zr–Zr distances d_1–d_4 in tetragonal $CoZr_2$ with the suggested gaussian distribution for amorphous $Co_{33}Zr_{67}$ (– – –) and the RDF determined by Steyer *et al.* [37] for amorphous $Co_{40}Zr_{60}$ (—; see text).

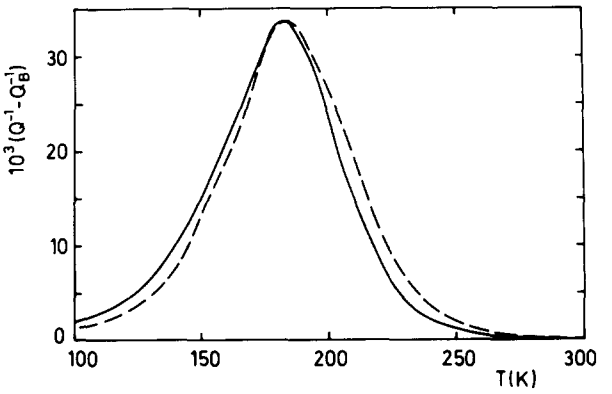

Fig. 6. Comparison of damping peaks at high H concentrations: —, amorphous $CoZr_2$, [H]/[M]=0.64, f=314 Hz; – – –, nanocrystalline $CoZr_2$, [H]/[M]=0.69, f=336 Hz [19].

a Zr–Zr radial distribution function (RDF) determined from X-ray data for amorphous $Co_{40}Zr_{60}$ [37].

Probing of the Co surroundings by occupation of Zr_3Co tetrahedra in amorphous $CoZr_2$, on the contrary, requires very high H concentrations in the [H]/[M] range between about 0.5 and 1 [8]. In that range, the IF peaks in the amorphous and nanocrystalline states (*i.e.* peaks 1 and 2′) appear almost identical not only in height and peak temperature but also in shape (Fig. 6).

Figure 7 shows the atomic arrangement around a Co atom in the cubic $E9_3$ structure. At the high H concentrations considered, there must be up to three protons around each Co atom, probably jumping between Zr_3Co tetrahedral sites with a strong mutual interaction. Here, the relaxation parameters can no longer reflect the geometry of single tetrahedra but probably the arrangement of all nine Zr atoms around a Co atom as a whole. The IF results seem to confirm the presumption [37] that this type of TSRO (distorted

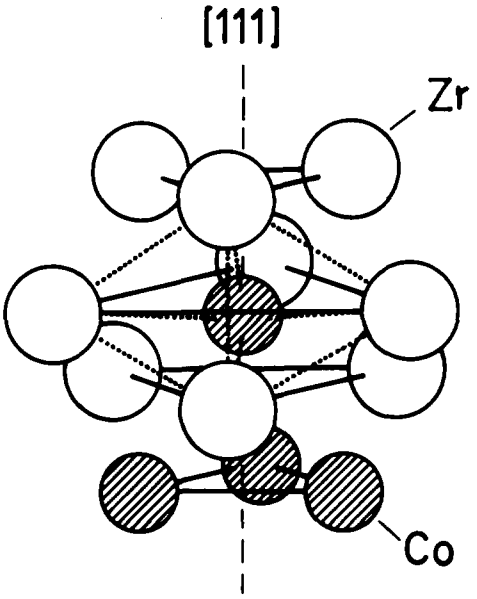

Fig. 7. The 12 neighbours of a Co atom in metastable, cubic $CoZr_2$, with indication of the trigonal symmetry (—; *cf.* ref. 37) and of a pair of Zr_3Co tetrahedra (· · · · ·).

trigonal prisms) around the Co atoms is also present in the amorphous structure.

In summarizing this example, MHS has revealed that the structure of amorphous $CoZr_2$ contains elements of short-range order from both the metastable cubic and the stable tetragonal crystalline phases. This might be an important finding for understanding the crystallization behaviour of this metallic glass, *e.g.* in terms of competing influences of Co–Zr and Zr–Zr interactions.

5. Other applications and outlook

Apart from the more sophisticated examples of the preceding sections that make use of the sensitivity of MHS to structural details in atomic dimensions, there are other applications on a more empirical basis suitable for characterizing the constitution and microstructure of a material on a larger scale. Here it is first of all the simple identification of a measured IF peak with a certain intermetallic phase that naturally gives rise to the application of MHS as a method for detecting phases and studying phase transformations.

For instance, sequences of IF spectra such as that in Fig. 1 may be used to follow directly the different phases forming and disappearing on the way from the amorphous state to thermodynamic equilibrium of the alloy $CoZr_2$. It has been pointed out previously [19, 38] that this method may be advantageous especially in those cases where microstructures and diffraction patterns are very complicated, as in the intermediate mixed state during the transformation sequence of $CoZr_2$. More systematic experiments of this kind are now planned in order to shed more light on the later stages of that complex crystallization sequence, especially on those processes that are responsible for the existence of the recently discovered, metastable hexagonal phase (see above).

A special case is the investigation of H-induced phase transformations where the hydrogen influencing the transformation behaviour can at the same time serve as a probe to detect the phases after the transformation. For instance, amorphous $CoZr_2$ containing several atomic per cent H partially transforms directly into the tetragonal equilibrium phase, as indicated by the appearance of the corresponding IF peak 4 [5, 38].

Further applications and a general improvement in the results that can be obtained with MHS in the sense of the present paper will depend on the progress made in future on the discovery, theoretical understanding and quantitative characterization of underlying relaxation processes. Since our knowledge of the reorientation relaxation in amorphous and, even more, in crystalline intermetallic phases is still in full development, the potential of MHS as a tool for structural investigations is certainly not yet exhausted.

References

1 O. Yoshinari and M. Koiwa, in L.B. Magalas and S. Gorczyca (eds.), *Mechanical Spectroscopy and its Applications in Materials Science*, Elsevier, Amsterdam, 1993, to be published.
L.B. Magalas and S. Gorczyca (eds.), *Proc. ECIFUAS-6, Mater. Sci. Forum, 119–121* (1993) 795.
2 F.M. Mazzolai, *Z. Phys. Chem., N.F., 145* (1985) 199.
3 B.S. Berry and W.C. Pritchet, in G. Bambakidis and R.C. Bowman (eds.), *Hydrogen in Disordered and Amorphous Solids*, Plenum, New York, 1986, p. 215.
4 B. Sobha, B. Coluzzi, F.M. Mazzolai, T.B. Flanagan and Y. Sakamoto, *J. Less-Common Met., 172* (1991) 254.
5 H.-R. Sinning, *J. Phys.: Condens. Matter, 3* (1991) 2005.
6 J. Buchholz, J. Völkl and G. Alefeld, *Phys. Rev. Lett., 30* (1973) 318.
7 G. Cannelli, R. Cantelli, F. Cordero and F. Trequattrini, *Mater. Sci. Forum, 119–121* (1993) 29.
8 J.H. Harris, W.A. Curtin and M.A. Tenhover, *Phys. Rev. B, 36* (1987) 5784.
9 R. Kirchheim, *Acta Metall., 30* (1982) 1069.
10 P.M. Richards, *Phys. Rev. B, 27* (1983) 2059.
11 U. Stolz, *J. Phys. F, 17* (1987) 1833.
12 B.S. Berry and W.C. Pritchet, *Z. Phys. Chem., N.F., 163* (1989) 381.
13 H. Mizubayashi, T. Naruse and S. Okuda, *Phys. Status Solidi A, 132* (1992) 79.
14 H.-R. Sinning, *Phys. Stat. Sol. A, 140* (1993) 97.
15 B.S. Berry, W.C. Pritchet and J.F. Bussière, *Scr. Metall., 17* (1983) 327.
16 O. Yoshinari, M. Koiwa, A. Inoue and T. Masumoto, *Acta Metall., 31* (1983) 2063.

17 B.S. Berry and W.C. Pritchet, in G.E. Murch, H.K. Birnbaum and J.R. Cost (eds.), *Nontraditional Methods in Diffusion*, Metallurgical Society of AIME, Warrendale, PA, 1984, p. 83.
18 H.-R. Sinning, *Phys. Rev. B, 46* (1992) 5989.
19 H.-R. Sinning and N. Matz, in A.R. Yavari (ed.), *Ordering and Disordering in Alloys,* Elsevier, London, 1992, p. 364.
20 H.-R. Sinning, *Mater. Sci. Forum, 119–121* (1993) 139.
21 H.-R. Sinning, *Phys. Status Solidi A, 131* (1992) 445.
22 W.B. Pearson, *Handbook of Lattice Spacings and Structures of Metals and Alloys*, Vol. 2, Pergamon, Oxford, 1967.
P. Villars, *Pearson's Handbook of Crystallographic Data for Intermetallic Phases,* American Society for Metals, Metals Park, OH, 1985.
23 U. Köster, T. Spassov and M. Sutton, in A. Conde, C.F. Conde and M. Millan (eds.), *Proc. 3rd Int. Workshop: Non-Crystalline Solids, Matalascañas, November 5–8, 1991, World Scientific*, Singapore, 1992, p. 149.
24 K.H.J. Buschow, *J. Less-Common Met., 85* (1982) 221; *J. Phys. F, 14* (1984) 593.
25 K. Jansson, M. Nygren and A. Östlund, *Mater. Res. Bull., 19* (1984) 1091.
26 Z. Altounian, E. Batalla, J.O. Ström-Olsen and J.L. Walter, *J. Appl. Phys., 61* (1987) 149.
27 M.M. Nicolaus, H.-R. Sinning and F. Haessner, *Mater. Sci. Eng. A, 150* (1992) 101.
28 H. Gleiter, *Prog. Mater. Sci., 33* (1989) 223.
29 R. Würschum, W. Greiner, R.Z. Valiev, M. Rapp, W. Sigle, O. Schneeweiss and H.-E. Schaefer, *Scr. Metall. Mater., 25* (1991) 2451.
30 C.U. Maier and H. Kronmüller, *Z. Metallk., 83* (1992) 12.
31 M.M. Nicolaus, *Doctoral Thesis*, TU Braunschweig, 1992.
32 P.H. Gaskell, in H. Beck and H.-J. Güntherodt (eds.), *Glassy Metals II*, Springer, Berlin, 1985, p. 5.
33 Ch. Hausleitner and J. Hafner, *Phys. Rev. B, 45* (1992) 115, 128.
34 G.A. Yurko, J.W. Barton and J. Gordon Parr, *Acta Crystallogr., 12* (1959) 909.
35 E.E. Havinga, *J. Less-Common Met., 27* (1972) 187.
36 R. Kirchheim, *Prog. Mat. Sci., 32* (1988) 261.
37 M. Steyer, H.-U. Krebs and H.C. Freyhardt, *Z. Phys. B, 66* (1987) 317.
38 H.-R. Sinning, M.M. Nicolaus and F. Haessner, *Mater. Sci. Eng. A, 133* (1991) 371.